

Structure and Nature of the Active Sites in CoMo Hydrotreating Catalysts Conversion of Thiophene

R. G. Leliveld, A. J. van Dillen, J. W. Geus, and D. C. Koningsberger

Department of Inorganic Chemistry, Debye Institute, University of Utrecht, P.O. Box 80083, 3508 TB Utrecht, The Netherlands
E-mail: leliveld@chem.ruu.nl

Received July 23, 1997; revised December 1, 1997; accepted December 1, 1997

The performance of sulfided (Co)Mo/alumina catalysts was studied in the conversion of thiophene between 423 and 773 K at atmospheric pressure. Reaction orders for thiophene, H₂, and H₂S were determined at several temperatures. The reaction order in thiophene increases with rising temperature, indicating a Langmuir-Hinshelwood mechanism. Beyond 550 K the conversion curve deviates from pseudo-first-order kinetics, demonstrating the influence of the surface coverage of thiophene on the reaction rate. Above 673 K the reaction rate rises exponentially with temperature which can be ascribed to the presence of a second type of active site that is only active at high temperatures. These catalytic data can be combined with recent structural studies using EXAFS spectroscopy to derive an activity-structure relation. It is proposed that at low temperature the active sites are terminal sulphur vacancies on the Co-promotor atom. In addition around 673 K a second type of sites becomes active, which is believed to consist of bridging sulphur vacancies in between Co and Mo atoms on the MoS₂ edges. © 1998

Academic Press

INTRODUCTION

Supported metal sulfide (MoS₂, WS₂) catalysts are extensively used in the hydroprocessing of oil feedstocks. To obtain a high activity industrial catalysts usually contain a promoter, such as Co or Ni. During the last decades an enormous number of papers have been published on the preparation and structure of these catalysts, the reaction mechanisms of HDS and HDN, the nature of the active sites, and the origin of the promotion effect of Co and Ni. For details on these subjects the reader is referred to some recent reviews (1–8).

Many studies dealt with the reaction kinetics and mechanism of thiophene HDS (7–10). In general, HDS reaction kinetics is described by Langmuir-Hinshelwood type of rate equations. H₂S is usually taken as an inhibitor in competition with thiophene for the same adsorption sites, while the adsorption of H₂ is assumed to take place on separate sites (11). Very interestingly, several authors reported a decrease of the apparent activation energy of the hydrogenolysis reaction at higher temperatures (12–15). This behavior, which

is particularly shown by Co-promoted catalysts, is ascribed to changes in the steady state surface coverage by thiophene (13, 15). In agreement with this, the reaction order of thiophene was observed to increase with rising temperature. Van Parijs and Froment (16) published a kinetic study in which they also investigated the subsequent hydrogenation of butenes to butane. The results indicated the existence of two types of active sites on HDS catalysts, one for hydrogenolysis and one for hydrogenation. Recently, Daage and Chianelli (17) proposed the “rim-edge” model with also two types of sites. In this model, hydrogenation only takes place on the so called “rim” sites at the top and bottom of MoS₂ stacks, while hydrogenolysis reactions occur on rim as well as edge sites.

Most authors assume the number of active sites on the sulfided catalysts to be constant and independent of the reaction temperature. However, recent radioisotopic studies on the exchange of labile sulfur in HDS catalysts question this assumption. Kabe and co-workers (18, 19) found that the amount of labile sulfur on the catalyst increases with reaction temperature as well as partial pressure of the reactant. Similar findings were reported by Massoth and Zeuthen (20). They suggested a varying distribution of mobile sulfur vacancies. Incorporation of a varying number of active sites can indeed lead to a better description of the catalytic behavior as demonstrated by Asua and Delmon (21) and Pille *et al.* (22).

In a recent study (23) we reported on an *in-situ* EXAFS study of the reaction of selenophene with sulfided (Co)Mo catalysts. Our results showed the existence of two types of sites. The first type is associated with terminal sulfur vacancies on promotor Co atoms; at high temperatures (673 K) also a second site involving sulfur vacancies bridging between Co and Mo atoms is observed. The objective of this paper is to present a study on the catalytic performance of (Co)Mo catalysts in the conversion of thiophene between 423 and 773 K and to discuss catalytic data in combination with our EXAFS results on the temperature dependence of the genesis and location of sulfur vacancies. The conversion of thiophene shows an increase in the reaction

rate above 673 K, accompanied by a rise of the apparent activation energy. A model is proposed that describes the nature of the active HDS sites at low and high temperatures and that explains the observed catalytic behavior over the whole temperature range.

METHODS

Preparation of the Catalysts

A 15 wt% MoO₃/γ-Al₂O₃ (further denoted Mo/Al₂O₃) catalyst was prepared by incipient wetness impregnation of preshaped bodies of γ-Al₂O₃ (Ketjen CK-300, specific surface area 200 m²/g, pore volume 0.63 ml/g) with an aqueous solution of (NH₄)₆Mo₇O₂₄ · 6 H₂O (Merck, p.a.) containing 25% ammonia. A γ-alumina-supported sample loaded with 3.8 wt% Co₃O₄ and 14 wt% MoO₃ (further denoted CoMo/Al₂O₃) was prepared by incipient wetness co-impregnation of γ-Al₂O₃ (Ketjen CK-300) with a solution containing the required amounts of (NH₄)₆Mo₇O₂₄ · 6 H₂O and Co(NO₃)₂ · 6 H₂O. All catalysts were dried first in an air flow for 4 h at 298 K, and then in static air at 383 K for 16 h. Subsequently, the samples were calcined in air at 723 K during 16 h. A commercial CoMo/Al₂O₃ hydrodesulfurization catalyst (KF742, further denoted com-CoMo/Al₂O₃) was obtained from Akzo Nobel Chemicals B.V. and used without further treatment.

Sulfidation and Catalytic Activity

Catalytic activity experiments were performed using an automated microflow apparatus. Weighed amounts of 50 to 750 mg of catalyst (sieve fraction 150–425 μm) were diluted with quartz powder (Merck p.a., sieve fraction 200–800 μm) to a total volume of 1.0 ml. For each experiment the mixture was placed in a quartz lab reactor (8 mm Ø). Prior to the HDS measurements the catalyst was sulfided in a 100 ml/min flow of H₂S/H₂/Ar (10/40/50) while the temperature was linearly raised from 298 to 793 K (5 K/min) and kept at this temperature for 30 min. Then the flow was switched to 50 ml/min of 2.4 vol% thiophene in H₂. Analysis of the reactor effluent was done using a gaschromatograph with a Chrompack CP-sil-5 CB column and a FID. The conversion of thiophene was measured at every 15 K at decreasing temperatures between 793 and 423 K at atmospheric pressure. The conversion was calculated according to Eq. [1] after checking that the response factors for all reaction products were the same within the limits of experimental accuracy:

$$\text{Conversion} = \frac{\sum_i \text{peak area product}_i}{\sum_i \text{peak area product}_i + \text{peak area thiophene}} \cdot 100\%. \quad [1]$$

The reaction orders of H₂, thiophene, and H₂S were measured at 533, 623, 673, and 773 K with the CoMo/Al₂O₃

samples. To measure under differential conditions the catalysts were diluted with quartz powder to achieve a conversion of thiophene of 15% at the chosen reaction temperature. The partial pressure of H₂ was varied between 4 and 80 vol% (2.4 vol% thiophene, 10 vol% H₂S, balance Ar). Similarly, the partial pressure of H₂S was varied between 10 and 20 vol% (2.4 vol% thiophene, 75 vol% H₂, balance Ar) and the partial pressure of thiophene was varied between 1.8 and 6.4 vol% (10 vol% H₂S, 80 vol% H₂, balance Ar), respectively.

Temperature Programmed Reduction

After thiophene conversion during 6 h at 673 K and cooling down to 298 K under a flow of thiophene/H₂/Ar temperature programmed reduction profiles of the catalysts were recorded (TPR-S). A 50 ml/min flow of H₂/Ar (45/5) was fed to the reactor, while the temperature was linearly raised from 298 to 873 K with 5 K/min. To monitor the reduction, the production of H₂S was recorded using an UV/VIS spectrophotometer (Varian, Quartz cuvetts Hellma, 20 mm) at λ = 232 nm.

RESULTS

The observed products of the conversion of thiophene were regular HDS products as cis-, trans-, 1-butene, n-butane, and H₂S. Negligible traces of iso-butane, iso-butene, butadiene, and tetrahydrothiophene were observed. To ensure that the conversion was not influenced by internal diffusion effects an experiment was performed with catalyst particles of a sieve fraction of 425–630 μm. The conversion was the same as measured with the 150–425 μm sieve fraction, indicating that internal diffusion limitation did not occur. External diffusion limitation was tested by measuring at two different linear gas velocities, but with the same space velocity. Since the conversion was not influenced, external diffusion limitation could be excluded as well.

Reaction Orders (323–773 K)

Table 1 contains the reaction orders measured in thiophene, H₂, and H₂S with the CoMo/Al₂O₃ catalyst at 533, 623, 673, and 773 K; experiments with the com-CoMo/Al₂O₃ gave similar results. The order in thiophene, as well

TABLE 1

Reaction Orders in the Thiophene Hydrodesulfurisation over CoMo/Al₂O₃

Temperature	Thiophene	Hydrogen	Hydrogen sulfide
533	0.5	0.8	-0.8
623	0.6	1.1	-0.7
673	0.7	1.2	-0.6
773	0.9	1.4	-0.4

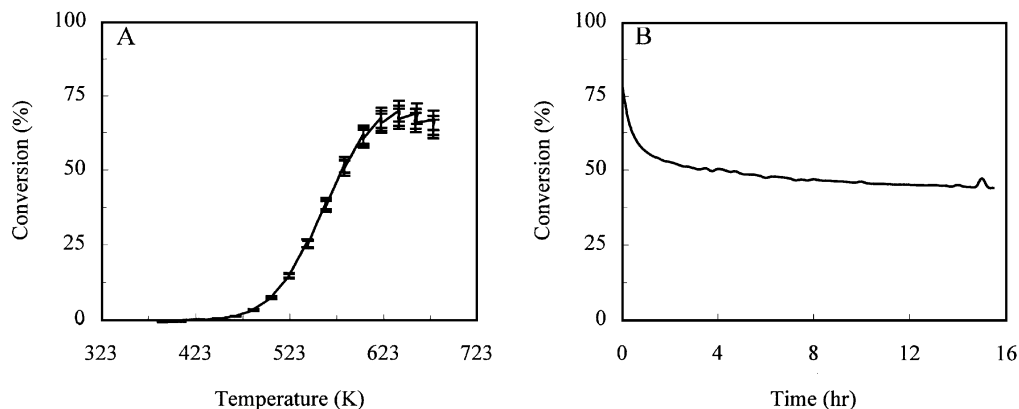


FIG. 1. (A) Conversion of thiophene for com-CoMo/Al₂O₃ at ascending temperature, space velocity 12000 h⁻¹, 50% H₂, 1.2% thiophene (estimated error ± 5%). (B) Conversion as a function of time after sulfidation at 673 K.

as the order in H₂, increased with rising temperature. The (negative) reaction order in H₂S increased with rising temperature, indicating less inhibition of the HDS reaction by H₂S at higher temperatures.

Thiophene Conversion (Influence of Space Velocity, 323–673 K)

To establish the effect of the contact time (τ) on the conversion curve experiments were performed with different space velocities. Figure 1A shows the performance of the commercial CoMo catalyst at a space velocity of 12000 h⁻¹ (space velocity calculated as the quotient of the flow rate and the catalyst volume), while heating the catalyst. Every 15 K three effluent samples were taken and analysed. As Fig. 1A shows, the conversion did not follow a simple first-order Arrhenius-like curve and it did not reach 100% conversion. The conversion even passed through a maximum at about 623 K and a conversion of 70%. Figure 1B displays the course of the conversion at 673 K as a function of the time on-stream of a freshly sulfided catalyst. It is clear that the catalyst deactivated from an initial conversion of 77% to a value below 50% after 16 h. Clearly, the

maximum in the conversion curve at 623 K (Fig. 1A) can be ascribed to a deactivation of the catalyst above this temperature. In order to avoid the influence of deactivation on the shape of the conversion curves, in further experiments the conversion was measured at descending temperatures after an initial stabilisation of the conversion during 6 h at the starting temperature of the experiment.

Figure 2 displays the conversion curves measured at descending temperatures for space velocities ranging from 1800 to 12000 h⁻¹. Despite previous stabilisation at 673 K, the conversion curves measured with the highest space velocities have an S-shaped form which does not agree with simple first-order kinetics. Figure 2B shows the Arrhenius curve based on an experiment in which the space velocity was 12000 h⁻¹. The curve was calculated from the conversion data for an integral reactor under the assumption of a pseudo-first-order relationship in thiophene and can be described according to

$$\ln \left[\ln \left[\frac{1}{1-x} \right] \right] = \ln[\tau \cdot k_0] - \frac{E_a}{RT} \quad [2]$$

in which x is the conversion, τ the contact time in the

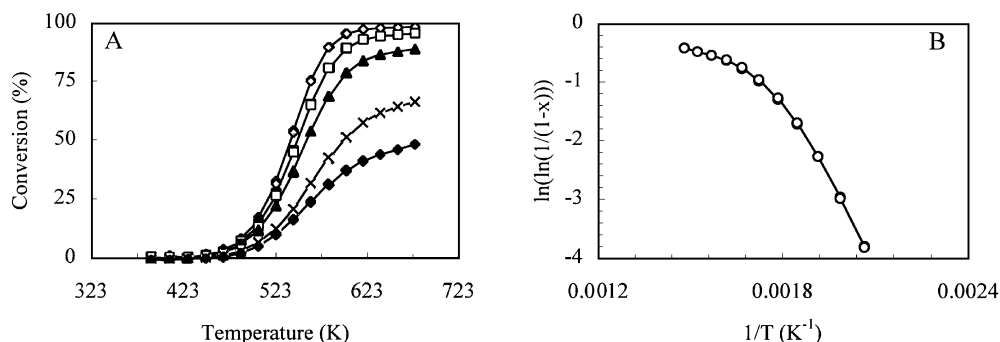


FIG. 2. (A) Conversion of thiophene for com-CoMo/Al₂O₃ at descending temperature, 50% H₂, 1.2% thiophene; space velocity 12000 h⁻¹, ◆; 6000 h⁻¹, ×; 3600 h⁻¹, open ▲; 2400 h⁻¹, □; 1800 h⁻¹, ◇. (B) Arrhenius curve for space velocity 12000 h⁻¹.

reactor, k_0 the preexponential factor, and E_a the apparent activation energy. The Arrhenius curve showed a decrease of the apparent activation energy from 85 ± 5 kJ/mol in the temperature range of 323–573 K to 15 ± 5 kJ/mol in the range of 573–673 K. A similar phenomenon could be observed when 10% H_2S was present in the feed and a space velocity of 1800 h^{-1} was chosen. The inhibiting effect of H_2S on the reaction rate shifted the conversion curve to higher temperatures, resulting in a curved Arrhenius plot similar to those obtained at higher space velocities without extra H_2S .

Thiophene Conversion (323–773 K)

The observed maximum in the conversion curves of lower than 100% made investigation of the catalytic behavior above 673 K interesting. Figure 3 displays the catalytic performance of $CoMo/Al_2O_3$. The measurements were done after stabilisation of the catalyst at 773 K for 6 h. Surprisingly, the conversion curves (depicted in Fig. 3A for a space velocity of 12000 h^{-1}) showed an increase in conversion around 700 K. After downward deviation from first-order kinetics around 600 K the conversion rose again above 700 K. The ascending and descending curves showed a hysteresis. At ascending temperatures the catalyst showed higher activity than at descending temperatures and even displayed a maximum in conversion at 630 K. Similarly, as shown in Fig. 3 the apparent activation energy shifted from 85 kJ/mol (450–550 K), to 15 ± 5 kJ/mol (600–675 K) and back to 33 ± 5 kJ/mol (710–785 K).

Figure 3C displays for the same experiment the conversion of the formed butenes into n-butane (conversion cal-

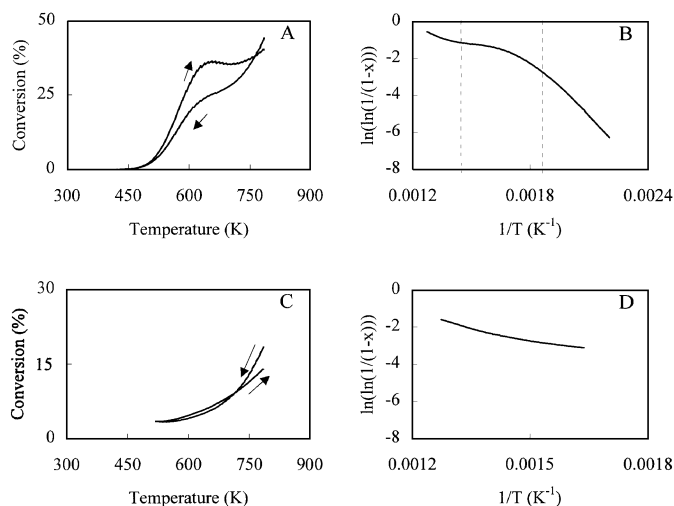


FIG. 3. (A) Conversion of thiophene for $CoMo/Al_2O_3$ at ascending and descending temperature, 90% H_2 , 2.4% thiophene, space velocity 12000 h^{-1} . (B) Arrhenius curve thiophene conversion (descending temperature). (C) Conversion of butenes for $CoMo/Al_2O_3$ at ascending and descending temperature, 90% H_2 , 2.4% thiophene, space velocity 12000 h^{-1} . (D) Arrhenius curve butene conversion (descending temperature).

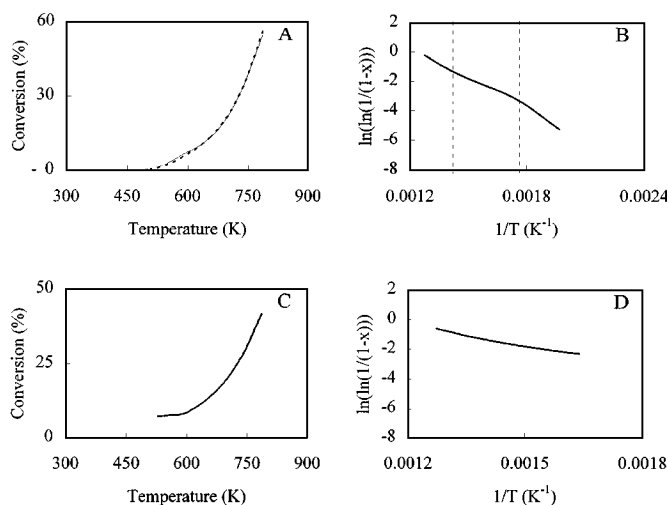


FIG. 4. (A) Conversion of thiophene for Mo/Al_2O_3 at ascending (solid line) and descending temperature (dotted line), 90% H_2 , 2.4% thiophene, space velocity 3000 h^{-1} . (B) Arrhenius curve of thiophene conversion (descending temperature). (C) Conversion of butenes for Mo/Al_2O_3 at descending temperature 90% H_2 , 2.4% thiophene, space velocity 3000 h^{-1} . (D) Arrhenius curve butene conversion (descending temperature).

culated similar to formula [1]), assuming that butane was only formed by hydrogenation of butenes. In contrast to hydrodesulfurisation of thiophene the conversion curve for hydrogenation followed a simple first-order Arrhenius-like trend. The apparent activation energy measured a value of 35 ± 5 kJ/mol. The conversion curves at ascending and descending temperatures were almost the same, especially below 700 K. The conversion at low temperatures did not reach zero, probably due to direct formation of butane from thiophene, without intermediate formation of butenes.

Figures 4A and B show the performance of the unpromoted Mo/Al_2O_3 catalyst and the accompanying Arrhenius curve. At first sight the conversion curve seemed to follow first-order kinetics. However, the Arrhenius curve did not prove to be a straight line. The apparent activation energy varied from 81 ± 5 kJ/mol (500–555 K) to 47 ± 5 kJ/mol (555–710 K) and back to 66 ± 5 kJ/mol (710–785 K). No hysteresis is observed between the two conversion curves as was observed with the promoted catalyst. The conversion of the formed butenes into iso- and n-butane is shown in Fig. 4C. Similar to the unpromoted catalyst, a straight Arrhenius plot was obtained (Fig. 4D) with an apparent activation energy of 39 ± 5 kJ/mol.

TPR of Sulfided Catalysts

In Fig. 5 the TPR-S patterns of the used catalysts, after thiophene conversion and cooling down to room temperature under HDS feed, are displayed. The pattern of the com- $CoMo/Al_2O_3$ catalyst exhibited four peaks at 400 K, 500 K, a shoulder at 600 K, and a broad peak starting at

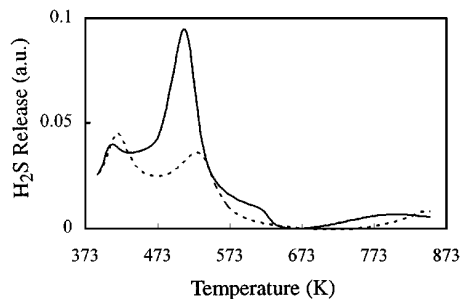


FIG. 5. TPR-S patterns of (A) com-CoMo/Al₂O₃ (solid line). (B) Mo/Al₂O₃ (dotted line).

673 K. The unpromoted Mo/Al₂O₃ catalyst showed a reduction behavior similar to that of the promoted catalyst, except for the absence of the shoulder at 600 K. The release of H₂S at high temperatures started at approximately 753 K.

DISCUSSION

Reaction Kinetics 323–773 K

The increase of the measured reaction order of thiophene with temperature definitely points to a Langmuir–Hinshelwood rate-controlled reaction as also found by other authors (11). Following the equation proposed by Satterfield and Roberts (24) and assuming that thiophene adsorption is in competition with H₂S on one type of site and that hydrogen adsorption takes place on a second type of site, the rate can be expressed as

$$r = k_r \frac{K_T P_T \cdot P_H}{(1 + K_T P_T + K_S P_S)} \quad [3]$$

in which r is the reaction rate, k_r is the reaction rate constant, K is the equilibrium constant, and P is the partial pressure (subscript T = thiophene, H = H₂, and S = H₂S). Assuming that the partial pressure of H₂S is constant (but still has a negative effect on the reaction rate), one can use the simpler equation

$$r = k_o \cdot e^{-(E_a/RT)} \cdot \frac{K P_T}{(1 + K P_T)} \cdot \frac{P_H^a}{P_S^b} \quad [4]$$

with

$$k_o = (kT/h) \cdot e^{-(S_a/R)} \cdot N_a, \quad [5]$$

$$K = A e^{-\Delta H_a/RT} \quad [6]$$

in which E_a is true activation energy, S_a is activation entropy, k is the Boltzmann constant, h is the Planck constant, N_a is the number of active sites, A is a preexponential factor, and ΔH_a is the energy of adsorption. The Arrhenius plot will lead to the following apparent activation energy (13):

$$E_{app} = E_a + \Delta H_a \frac{\Delta H_a K P_T}{1 + K P_T} \quad [7]$$

At low temperatures the surface coverage of thiophene is high ($K \cdot P_T \gg 1$), leading to a relatively low reaction order and an activation energy equal or near to the true activation energy. At higher temperatures the surface coverage gradually decreases, the reaction order in thiophene rises to a limiting value of 1, and the slope of the Arrhenius curve decreases.

To study the effect of a decreasing surface coverage on the shape of the conversion curve theoretical conversion curves were calculated using the above rate equations. For an integral reactor (varying partial pressure of thiophene) the conversion can be calculated according to

$$x = 1 - \exp\left(-k' \cdot \exp\left(\frac{-E_a \cdot \tau}{RT}\right)\right) \quad \text{with } k' = k_o \cdot \frac{P_H}{P_S} \quad [8]$$

In Fig. 6A, curve I is drawn, assuming first-order kinetics over the whole temperature range. This curve was constructed from the experimental conversion curve by extraction of k' and E_a from the low-temperature part of the experimental Arrhenius plot. Around 550 K the experimental curve starts to deviate from the calculated one due to a decrease of the surface coverage with thiophene. Curve II represents the surface coverage θ calculated according to Eq. [9] with realistic values for the adsorption energy and

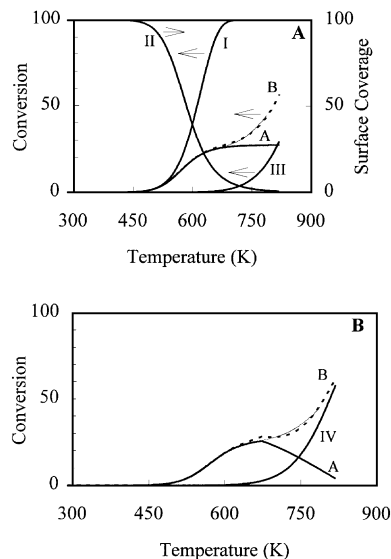


FIG. 6. (A) Experimental conversion of thiophene for CoMo/Al₂O₃ at descending temperature, 90% H₂, 2.4% thiophene, space velocity 12000 h⁻¹ together with (see Table 2) exponential curve (I), surface coverage (II), exponential curve type II sites (III), simulated conversion curve including surface coverage (A) and simulated conversion curve including curves A and III (curve B, dotted line). (B) Like Fig. 6a, exponential curve type II sites (IV), simulated conversion curve including surface coverage and decreasing number of active sites (curve A) and sum curves A and IV (curve B, dotted line).

TABLE 2
Mathematical Parameters Used in the Simulated Conversion Curves

Curve	E_a^a	k'	ΔH_a^a	A
I	85	4.2e7		
II			85	2.5e-8
III	110	1.2e7		
IV	110	3.0e7		

^a In kJ/mol.

the pre-exponential factor (see Table 2):

$$\Theta = \frac{K \cdot P_T}{1 + K \cdot P_T} \quad [9]$$

To calculate the conversion curve, taking into account the decreasing surface coverage, the reaction rate was calculated according to Eq. (4), leading to

$$r = \frac{dp}{dt} = k' \cdot \frac{K \cdot P_T}{1 + K \cdot P_T} \quad [10]$$

To calculate the thiophene partial pressure at the end of the reactor one can either solve Eq. [10] by integrating over the contact time τ or, as we choose, use a numerical approach. In the latter the reactor was divided into 10 segments in which the thiophene concentration was assumed constant. The thiophene partial pressure at the end of each segment could easily be obtained by using Eq. [10]. As input value for the thiophene pressure P_T the outlet concentration of the former segment was used etc. As shown in Fig. 6A the experimental curve can then be simulated up to a temperature of almost 673 K (curve A). Above 673 K the calculated conversion does not rise anymore with the temperature; however, experimentally an increase of the conversion is observed. According to the Langmuir–Hinshelwood relation, the surface coverage decreases to very low values at these temperatures ($K \cdot P_T \ll 1$) and the increase in the reaction rate constant due to the rising temperature is compensated. As a consequence, the conversion becomes more or less temperature independent (curve A at high temperature). At some point the steady-state surface coverage will be even so low that one can speak of an Eley–Rideal type of mechanism in which the collisions between gas molecules and the catalyst surface are rate determining. Clearly, these calculations demonstrate that the observed increase of the conversion above 673 K cannot be explained by the presence of one type of hydrogenolysis sites with a Langmuir–Hinshelwood type of kinetics.

To be able to completely describe the experimental curve, a second type of active sites with a higher activation energy has to be implemented (curve III, calculated according to Eq. [8]). Taking into account this second type of sites, the

shape of the experimental curve can be completely simulated as is demonstrated by curve B, that is the sum of curves A and III.

Finally, the used rate equations imply a negative reaction for hydrogen sulfide as, indeed, observed and a value of maximal 1.0 for the order in hydrogen. However, the values of 1.2 and 1.4 found at high temperatures are well above 1.0 and no satisfying explanation can be given to explain these results.

Evidence for Two Types of HDS Sites

The TPR-S pattern of the spent catalyst shows two peaks, one at low and one at high temperatures. The peak at low temperatures has been ascribed by Moulijn and co-workers (25, 26) to sulfur that is chemisorbed on coordinative unsaturated Co and/or Mo atoms at the edges of the MoS₂ slabs. The observed release of H₂S above 673 K in the TPR-S proves that hydrogenation of more strongly bonded sulfur atoms proceeds beyond this temperature. Most likely these are stoichiometric sulfur atoms, such as the bridging sulfur atoms that are part of the edge structure of the MoS₂ slabs (27).

In a recent study we reported on the adsorption of selenophene on the active sites in sulfided (Co)Mo catalysts studied with EXAFS (23). The results showed that at 473 K the active sites can be considered to be the terminal sulfur vacancies of the promotor Co atoms as depicted in Fig. 7A. At 673 K the EXAFS analysis revealed that, in addition, Se had also been incorporated at the positions of the bridging sulfurs between the Mo and Co atoms at the MoS₂ edges (see Fig. 7B).

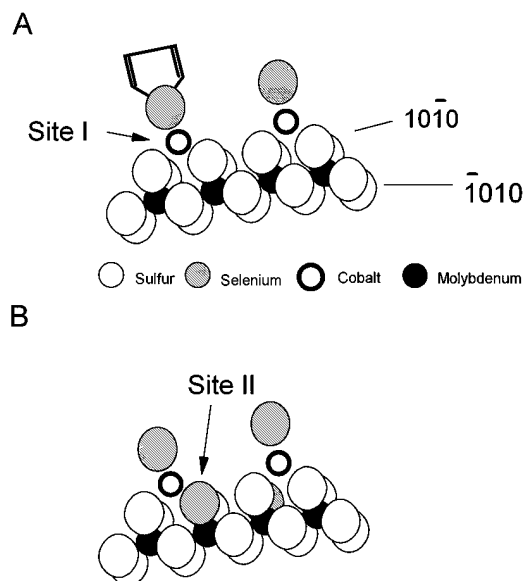


FIG. 7. Structure of CoMo/Al₂O₃ catalyst after reaction with selenophene as determined with EXAFS (A) 473 K, (B) 673 K.

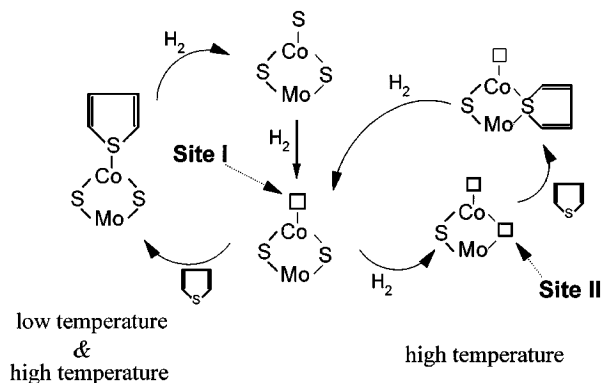


FIG. 8. Reaction scheme for thiophene HDS at low and high temperature.

Combining the outcome from the reaction kinetics experiments with both the TPR-S and EXAFS results leads to a structure–activity relation. All results clearly point to the presence of two types of active HDS sites. As shown in Fig. 8, at low temperatures (possibly also at higher temperatures) the reaction occurs exclusively on terminal sulfur vacancies on the Co atoms (Type I), while at high temperatures (around and above 673 K) the HDS of thiophene also proceeds on the bridging sulfur vacancies between Co and Mo (Type II). The Type II sites are only active when the temperature is sufficiently high for hydrogenation of the bridging sulfurs to take place, represented by the high temperature peak in TPR-S. The EXAFS results confirm that Se is only found in this bridging position after reaction at 673 K and not at 473 K. Sites I and II, from which site II is only active at high temperature, explain the observed catalytic behavior over the whole temperature range of 423–793 K.

Additionally, it has to be mentioned that there might be an alternative explanation for the type-II EXAFS site. It may be that at high temperatures a redistribution of the S and Se atoms takes place within the Co–Mo–S structure. This may lead to the observation with EXAFS that Se is in the bridging position between Co and Mo, although the initial adsorption and HDSe of selenophene took place at the terminal Co position. In that case, however, there must still be a second site for thiophene HDS which we cannot yet describe.

Analysis with EXAFS of the CoMo catalyst showed that in the terminology of CoMoS I and CoMoS II the CoMoS phase in this catalyst can be described as CoMoS II, i.e. no chemical linkages between the alumina-support surface and the CoMoS phase. All the Co atoms are also in a similar environment, indicated by the Co–Mo coordination of 1.0. This means that the two types of active sites are not related to CoMoS I or II since this catalyst only contains one sort of those. The two types of sites have thus to do with two kinds of sulfur vacancies, instead of two kinds of CoMoS phases, as is also indicated by the existence of two types of sites in the unpromoted Mo catalyst.

Participation of Low Temperature Site at Temperatures > 673 K

A point of consideration is the participation of site I (on the Co atoms) at higher temperatures. It might well be that these sites are inoperative at high temperatures, for example, due to the removal of the bridging sulfurs that are in the coordination sphere of the same Co atom. Our data do not allow to draw a definite conclusion. Figure 6B represents a conversion curve that is constructed assuming a decrease of the number of type-I sites starting at 673 K of $\Delta k_0 = 2.5 \times 10^5/\text{K}$ (curve A). In order to follow the course of the experimental curve the calculated conversion curve is based upon an increasing number of type-II sites (curve IV). It is clear that certainly more than one mathematical solution will fit the experimental curve, all yielding different preexponential factors and activation energies. Moreover, it is not clear whether a Langmuir–Hinshelwood-type of rate equation should be used for the type-II site. In other words, the extent of the contribution of ΔH_a (for adsorption on the type-II site) to the apparent activation energy of these sites (in the range of 673–773 K) is not known. The order in thiophene of 0.9 at 773 K indicates the surface coverage to be low and a significant contribution of ΔH_a can be expected. However, we feel that with this data set it is no use to implement the surface coverage for the second type of sites here since no unique mathematical solution can be found anyhow.

Activity of the High Temperature Site

The EXAFS results showed site II already at 673 K, while the H₂S release in the TPR-S pattern, creating site II, is observed to start at higher temperatures. Additionally, the amount of H₂S released above 673 K is small, compared to the low temperature peak, suggesting that the number of type-II sites is low. As Kabe and co-workers (19) reported in their studies with ³⁵S-labelled dibenzothiophene, at 633 K no release of H₂S from the catalyst was observed unless dibenzothiophene was present in the feed. This implies the occurrence of a concerted mechanism in which the release of H₂S is directly coupled to the adsorption and HDS of the reactant, the latter being the rate-determining step(s). In our TPR experiments the metal sulfide releases sulfur as H₂S without the presence of “fresh” sulfur in the feed. For these reasons one may expect that the temperature at which a sulfur atom is released as H₂S during TPR can be much higher than needed for the genesis of an active site (note also that there is a small difference in the H₂ partial pressure of 0.9 in the catalytic tests versus 1.0 in the TPR-S results). Additionally, the amount of released sulfur with TPR does not necessarily have to correspond to the number of vacancies active during HDS and will probably be much smaller since no “fresh” sulfur is present to directly fill the created vacancies. The number of active sites is determined

by the hydrogenation rate of labile sulfur atoms, resulting in vacancies followed or induced by simultaneous adsorption of the reactant.

Actually, in our model of the type-II site as the bridging vacancy between Co and Mo, a concerted mechanism has to be assumed. Otherwise, removal of the bridging sulfur will lead to a collapse of the Co–Mo–S structure, due to the fact that the Co will then become threefold coordinatively unsaturated, which situation is not likely to be stable.

Interconversion of the Two Catalytic Cycles

As described above it is clear that two catalytic cycles are operative and that their working temperatures overlap to an extent that is unknown. In view of this, the hysteresis between the conversion curves at ascending and descending temperatures is interesting. The curve measured with rising temperatures is well above the conversion curve measured with decreasing temperatures and even shows a maximum at around 620 K. It is expected that the equilibrium between adsorbed and gaseous thiophene is quickly reached and does not influence the shape of the curve. It is therefore tempting to assume that above 610 K (ascending curve) the number of active sites (the preexponential factor) starts to decrease, resulting in the observed maximum in the conversion. As discussed above, this might be caused by the removal of sulfur atoms from site II, which kills site I on the Co atom. When the temperature is decreased it takes time to restore the original sulfide structure (assuming that the process is completely reversible), resulting in a lower activity compared to the conversion curve measured with increasing temperatures. The hysteresis between the two curves can thus be explained by a nonequilibrium state of the structure of the sulfided catalyst.

Unpromoted Catalyst

As shown in Fig. 4, the unpromoted catalyst displays a behavior similar to that of the promoted catalyst, although much less pronounced. The activation energy at low temperatures is about equal to that of the promoted catalysts: 85 versus 81 kJ/mol, respectively. The large difference in activity (compare space velocity $3000 \text{ h}^{-1} \text{ Mo/Al}_2\text{O}_3$ versus 12000 h^{-1} for $\text{CoMo/Al}_2\text{O}_3$) can thus mainly be ascribed to a different preexponential factor or number of active sites. In analogy to the promoted catalyst the EXAFS experiments (23) showed that at 673 K S is incorporated in positions of bridging sulfur atoms at the MoS_2 edge (site II). At lower temperature it is reasonable to assume that the reaction can also proceed over terminal sulfur vacancies that are present on the $10\bar{1}0$ plane.

Additionally, no hysteresis is observed between the two conversion curves measured with increasing and decreasing temperatures. This suggests that the structural rearrangements, necessary to restore the low temperature sites, are faster on the unpromoted catalyst than on the promoted

catalysts. Alternatively, one may argue that the number of low temperature sites on sulfided $\text{Mo/Al}_2\text{O}_3$ is quite limited due to the anchoring of the $10\bar{1}0$ plane to the support (or that terminal sulfur vacancies are not very active!). The activity of unpromoted catalysts can then mainly be ascribed to the vacancies on bridging sulfur sites at the MoS_2 edges. This is partly supported by the TPR-S measurements of Scheffer *et al.* (28) who showed that the amount of chemisorbed sulfur removable at low temperature, normalised per Mo atom, increased substantially when $\text{Mo/Al}_2\text{O}_3$ catalysts were promoted with Co.

Hydrogenation Sites

Interestingly, the Arrhenius curve for the hydrogenation of the butenes into butanes is only slightly curved which is quite different from the hydrogenolysis reaction. This might imply that the active sites for hydrogenation and HDS are different sites as already pointed out by several authors (16, 22, 29). Wambeke *et al.* (30) argued in their study on unpromoted $\text{MoS}_2/\text{Al}_2\text{O}_3$ catalysts that the hydrogenation sites are threefold-coordinatively unsaturated molybdenum ions in the $\bar{1}010$ plane. In their extensive review, Topsøe *et al.* (8) discuss the activation of hydrogen and the importance of SH groups. In their view SH groups are related to the MoS_2 structure and are available to donate hydrogen at positions close to the promotor atoms. It is generally accepted that activation of hydrogen (homolytically or heterolytically) takes place on coordinatively unsaturated sites under the formation of SH groups (31–33). To create these triple CUS sites edge sulfur atoms have to be removed, which might suggest that the hydrogenation site is similar to type-II sites that are active at high temperatures (for instance, the corner sites) or possibly the same site. In any case, the similarity between the promoted and unpromoted catalyst in the conversion of butenes support location of the hydrogenation sites on the MoS_2 phase.

CONCLUSIONS

The conversion of thiophene was studied for sulfided (Co)Mo/Al₂O₃ catalysts in the temperature range of 423 up to 773 K at atmospheric pressure. The following conclusions can be drawn:

—The reaction order in thiophene increases with increasing temperature, indicating a Langmuir–Hinshelwood mechanism. Incorporating the surface coverage into the rate equation enables a description of the experimental conversion curve up to 673 K.

—Above 673 K the reaction rate shows an increase that can no longer be described by a rate equation based upon one type of active sites (site I). However, incorporation of a second type of sites (site II), active at high temperatures, explains the observed behavior.

—On the basis of earlier reported EXAFS results we propose that the two types of active sites can be associated with terminal vacancies located on the terminal sulphur position on the promotor Co atoms (site I) and with edge vacancies located on the position of bridging sulphur atoms in between Co and Mo atoms on the MoS₂ edges (site II), respectively. The latter site only becomes active at temperatures near or above 673 K.

—The hydrogenation of butenes into butane obeys simple first-order kinetics and is assumed to operate over one type of active sites, located on the MoS₂ phase. However, although the HYD conversion has the same behavior as a function of temperature for both Mo and CoMo catalysts the absolute levels of conversion are very different.

REFERENCES

1. Ratnasamy, P., and Sivasanker, S., *Catal. Rev.-Sci. Eng.* **22**, 401 (1980).
2. Keely, W. M., Jerus, P., Dienes, E. K., and Hausberger, A. L., *Catal. Rev.-Sci. Eng.* **26**, 485 (1984).
3. Dellanay, F., *Appl. Catal.* **16**, 135 (1985).
4. Prins, R., de Beer, V. H. J., and Somorjai, G. A., *Catal. Rev.-Sci. Eng.* **31**, 1 (1989).
5. Breysse, M., Portefaix, J. L., and Vrinat, M., *Catal. Today* **10**, 489 (1991).
6. Chianelli, R. R., Daage, M., and Ledoux, M. J., *Adv. Catal.* **40**, 177 (1994).
7. Startsev, A. N., *Catal. Rev.-Sci. Eng.* **37**, 353 (1995).
8. Topsøe, H., Clausen, B. S., and Massoth, F. E., in "Catalysis-Science and Technology," Vol. 11. Springer-Verlag, New York/Berlin, 1996.
9. Vrinat, M. L., *Appl. Catal.* **6**, 137 (1983).
10. Girgis, M. J., and Gates, B. C., *Ind. Eng. Chem. Res.* **30**, 2021 (1991).
11. Radomyski, B., Szczygiel, J., and Trawczynski, J., *Appl. Catal.* **39**, 25 (1988).
12. Morooka, S., and Hamrin, C. E., *Chem. Eng. Sci.* **32**, 125 (1977).
13. Gellman, A. J., Neiman, D., and Somorjai, G. A., *J. Catal.* **107**, 92 (1987).
14. Startsev, A. N., Shkuropat, S. A., and Bogdanets, E. N., *Kinet. Catal.* **35**, 258 (1994).
15. Leglise, J., van Gestel, J., and Duchet, J. C., *Prep. ACS* **39**, 533 (1994).
16. Van Parijs, I. A., and Froment, G. F., *Ind. Eng. Chem. Prod. Res. Dev.* **25**, 431 (1986).
17. Daage, M., and Chianelli, R. R., *J. Catal.* **149**, 414 (1994).
18. Qian, W., Ishihara, A., Ogawa, S., and Kabe, T., *J. Phys. Chem.* **98**, 907 (1994).
19. Kabe, T., Qian, W., Wange, W., and Ishihara, A., *Catal. Today* **29**, 197 (1996).
20. Massoth, F. E., and Zeuthen, P., *J. Catal.* **145**, 216 (1994).
21. Asua, J. M., and Delmon, B., *Appl. Catal.* **12**, 249 (1984).
22. Pille, R. C., Yu, C.-Y., and Froment, G. F., *J. Mol. Catal.* **94**, 369 (1994).
23. Leliveld, R. G., van Dillen, A. J., Geus, J. W., and Koningsberger, D. C., *J. Phys. Chem. B*, in press.
24. Satterfield, C. N., and Roberts, G. W., *AIChEJ* **14**, 159 (1968).
25. Scheffer, B., Dekker, N. J. J., Mangus, P. J., and Moulijn, J. A., *J. Catal.* **121**, 31 (1990).
26. Mangus, P. J., Riezebos, A., van Langeveld, A. D., and Moulijn, J. A., *J. Catal.* **151**, 178 (1995).
27. McGarvey, G. B., and Kasztelan, S., *J. Catal.* **148**, 149 (1994).
28. Scheffer, B., Dekker, N. J. J., Mangnus, P. J., and Moulijn, J. A., *J. Catal.* **121**, 31 (1990).
29. Okamoto, Y., Maezawa, A., and Imanaka, T., *J. Catal.* **120**, 29 (1989).
30. Wambeke, A., Jalowiecki, L., Kasztelan, S., Grimblot, J., and Bonelle, J. P., *J. Catal.* **109**, 320 (1988).
31. Jalowiecki, L., Grimblot, J., and Bonelle, J. P., *J. Catal.* **126**, 101 (1990).
32. Polz, J., Zellinger, H., Muller, B., and Knözinger, H., *J. Catal.* **120**, 22 (1989).
33. Anderson, A. B., Al-Saigh, Z. Y., and Hall, W. K., *J. Phys. Chem.* **92**, 803 (1988).